Continuous Measurement of Dynamic Tensile Mechanical Properties in Polymer Solids over a Wide Range of Frequencies. I. An Instrument with Driving Force of 15 kgwt and Frequency Range 10^{-3}–10^{2} Hz

MITSURU YOKOUCHI and YASUJI KOBAYASHI, *Department of Industrial Chemistry, Faculty of Technology, Tokyo Metropolitan University, Fukazawa, Setagaya-ku Tokyo 158, Japan*

Synopsis

Two compact apparatuses were designed and fabricated for the study of dynamic mechanical viscoelastic behavior in polymer solids over a wide range of frequencies: (1) 10^{-3}–10^{2} Hz with a tensile driving force of 15 kgwt, and (2) 10–10^{4} Hz with a maximum tensile driving force of 15 kgwt. The present paper reports the details of the instrument of (1). The instrument contains a nonresonant and forced vibration system, where the rectilinear vibration is taken from the rotating shaft of the driving motor through the double eccentric crank and conrod-slider machineries. Measurements can be conducted at any desirable frequency (10^{-3}–10^{2} Hz) and displacement (0–2 mm). Subjected to longitudinal vibration, the stress and strain in the specimen are detected by a compression-type load cell and noncontacting displacement meter, respectively. The specimen clamp was especially devised for the compression-type load cell, which enables direct conversion from the tensile force on the specimen to the compressive force against the load cell without any medium. Another feature of the instrument is a vertical combination of vibrational driving system, specimen clamp, and load cell. These are important for the effective transmission of the driving force to the specimen and avoidance of unnecessay mechanical vibration noises. From the Lissajous' figure formed with two signals of the stress and strain, the values of dynamic tensile modulus and loss factor for polymeric materials are easily obtained.

INTRODUCTION

Molecular motion is one of the important factors governing the physical properties of polymeric materials. This is diversified due to their large molecular weights and complicated structures. There are two types of experimental methods for the study of molecular relaxation in polymer solids: (1) measurement of molecular fluctuations at external force-free state, and (2) measurement of the response (viscoelastic behavior) when a polymer solid receives an external force and its molecular motions are disturbed. Our attention is focused on the latter case, especially, when subjected to dynamic tensile force.

Generally, the dynamic viscoelastic properties of polymer solids are known as functions of temperature and frequency. Regarding temperature dispersion at a constant frequency (mostly 110 Hz), many studies have been conducted. However, the data for frequency dispersion have been minimal until now. If the temperature–frequency superposition principle is not affected, the data for frequency and temperature dispersion are necessary for accurate understanding of the dynamic mechanical viscoelastic properties. Furthermore, in the high-

Journal of Applied Polymer Science, Vol. 26, 4307–4315 (1981)
 CCC 0021-8995/81/124307-09$01.00

speed and light-weight inclinations, the former data on plastics and rubbers will be increasingly demanded.

For the measurement of dynamic mechanical properties, some apparatuses have already been commercialized. There are several weak points in their performance: (1) sinusoidal driving force is small; (2) frequency range is narrow and discrete. Overcoming the above faults and adopting a new idea, we established a measuring system for the frequency dispersion over a wide range of frequencies (10^{-3}–10^4 Hz) with two compact instruments (10^{-3}–10^2 and 10–10^4 Hz). The present report describes the detailed procedures of design and fabrication for the former instrument (10^{-3}–10^2 Hz) and its application to some polymers.

PRINCIPLE

When subjected to the tensile external force σ, a viscoelastic material responds with the displacement ϵ and phase lag δ as shown in Figure 1. The fundamental relationships are as follows:

$$\text{tensile load } \sigma = A \sin(f2\pi t) \tag{1}$$

$$\text{displacement } \epsilon = B \sin[f(2\pi t + \delta)] \tag{2}$$

$$\text{velocity } v = -2\pi fB \cos(f[2\pi t + \delta]) \propto -2\pi fB \tag{3}$$

$$\text{acceleration } \alpha = 4\pi^2 f^2 B \sin(f[2\pi t + \delta]) \propto 4\pi^2 f^2 B \tag{4}$$

where A and B are the amplitudes of load and displacement, respectively, and f is frequency. Then the complex modulus may be stated by eqs. (5) and (6):

$$\text{dynamic tensile storage modulus } E' = A \frac{\cos\delta}{S \ln[1 + (B/L)]} \tag{5}$$

$$\text{dynamic tensile loss modulus } E'' = A \frac{\sin\delta}{S \ln[1 + (B/L)]} \tag{6}$$

where S and L are the cross section and length of the specimen, respectively. When σ and ϵ are observed, the values of A, B, and δ can be easily obtained and, furthermore, so can E' and E''.

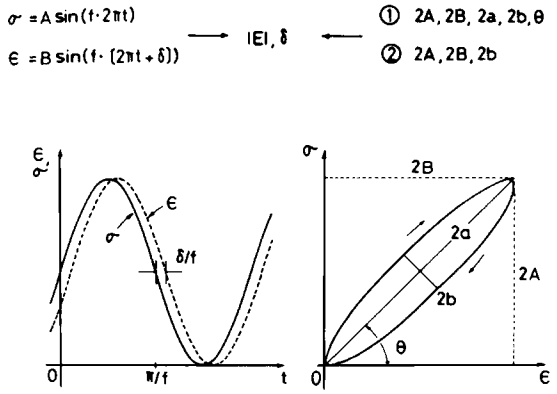

Fig. 1. Sinusoidal stress–strain curve and its Lissajous' figure. With high precision, the complex modulus data are obtained from the three reading parameters $2A$, $2B$, and $2b$.

INSTRUMENT

The instrument described herewith consists of the following three elements: (1) sinusoidal driving force assembly, (2) load cell and specimen clamp, and (3) recording device. In order to obtain meaningful and characteristic sinusoidal stress–strain curves, a few problems should be resolved: (1) sufficient driving force during the entire frequency range, (2) no distortion of sinusoidal driving force, and (3) eliminate unnecessary mechanical vibration noises which prevent continuous measurements.

Sinusoidal Driving Force

In order to measure dynamic tensile viscoelastic properties at any frequency between 10^{-3} and 10^{2} Hz, a resonant vibration method is inconvenient because a special specimen shape is necessary and its resonant frequency changes with temperature. Therefore, the measurement of frequency dispersion necessitates the forced and nonresonant vibration method. As proper drivers, electrodynamic vibrators (a kind of speaker with large power) have been generally utilized.[1,2] In spite of the easy control of frequency and clear wave of sinusoidal driving force, they have a fundamental fault, i.e., insufficient driving force. The driving force of electrodynamic vibrators F is estimated as follows using eq. (4):

$$F = (m_1 + m_2 + m_3)4\pi^2 f^2 B \tag{7}$$

where m_1 is a mass of the moving coil and bobbin in the driver, m_2 is the mass of the fixture containing the specimen clamp, and m_3 is the mass of the specimen, respectively. The dynamic measurement becomes possible when the driving force is larger than the tensile load σ:

$$F > \sigma \tag{8}$$

When, for example, $(m_1 + m_2 + m_3)$ is 1 kg and B is constant at 100 μm, the

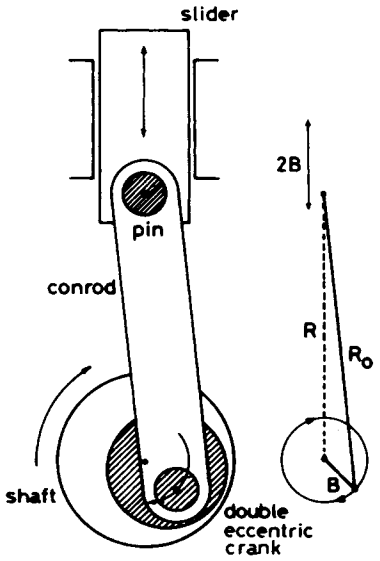

Fig. 2. Sinusoidal driving force machinery with motor.

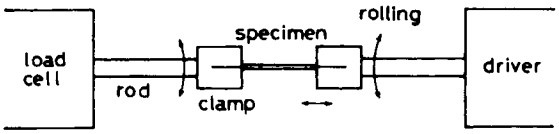

Fig. 3. Conventional clamping method for the specimen.

driving force F changes from 4×10^{-9} N to 4×10 N in the range 10^{-3}–10^{2} Hz. In the lower frequency range, even a higher-power electrodynamic vibrator (m_1 is heavier) cannot easily satisfy eq. (8). To compensate for this insufficiency, electrohydraulic vibrators have been developed. Their apparatuses, however, are large and expensive. Furthermore, the generation of the clear sinusoidal driving force is relatively difficult. Our object was to fabricate a compact instrument with high performance. Therefore, we adopted a motor as a driver; its driving force is governed by its torque. A rotating motion of the motor's shaft is converted to the reciprocating motion through a double-eccentric crank and conrod-slider (Fig. 2). The distance from the pin to the center of the rotating shaft R is given as follows by the use of the length of conrod R_0:

$$R = B \sin\phi + (R_0^2 - B^2 \cos^2 \phi)^{1/2} \tag{9}$$

$$\fallingdotseq B \sin\phi + R_0 \qquad R_0 \gg B \tag{10}$$

Then, the displacement is represented by

$$\epsilon = \Delta R = B \sin(f2\pi t) \tag{11}$$

where $\phi = f2\pi t$.

The stroke $2B$ can be easily and continuously adjusted by the double-eccentric crank. In the approximation from eq. (9) to eq. (10), the deviation is very small (e.g., maximum 0.3% when R_0 is 30 mm and B is 2 mm). From this estimation, the distortion can be almost ignored when precision miniature bearings are used.

Load Cell and Specimen Clamp

Thus far, the force of one end of the specimen has been detected by a tension-type load cell which is fixed to the specimen clamp through a long and heavy connecting rod (Fig. 3). This rod is very harmful to the vibration system since it causes a mechanical vibration noise, especially during rolling vibration due to its length. This resonance prevents continuous frequency dispersion measurements. Secondly, the driving force cannot be effectively transmitted to the specimen due to its weight. [eq. (7)]. Even when the driver has sufficient power to vibrate the specimen, it is insufficient at the higher frequency range because of the abundant mass of the connecting rod. The removal of this rod may enlarge the applicability of electrodynamic vibrator as a driver. In order to resolve this problem, we devised a new clamping method for the specimen and a detecting method for the load. A compression-type load cell was utilized as a load sensor because of its higher natural frequency. The dynamic range of the load cell is from 3 gwt to 3000 gwt. Next, a proper method was sought where a tensile load on the specimen could be converted to a compressive force against the load cell without any medium. A specimen clamp was considered to serve both purposes of the above machinery and the clamping of the specimen (Fig. 4). This clamp,

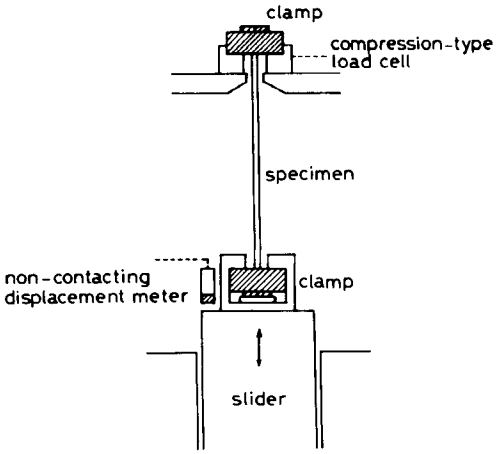

Fig. 4. Vertical combination of the specimen's clamp, the compression-type load cell, and the driver.

TABLE I
Specimens for Performance Testing

Specimen	Density	Crystallinity	Birefringence
PE			
a (Undrawn)	—	—	—
b (Rolled ×2)	0.962	0.78	—
c (Rolled ×3)	0.962	0.78	—
d (Rolled ×6)	0.965	0.79	0.007
e (Uniaxially ×6)	0.965	0.79	0.018
f (Uniaxially ×8)	0.965	0.79	0.031
PET			
a (Undrawn)	1.344	0.07	—
b (Uniaxially ×2)	1.344	0.07	0.007
c (Uniaxially ×3)	1.354	0.16	0.031
d (Uniaxially ×3.8)	1.365	0.25	0.064

made of duralumin or fiber-reinforced plastic (FRP), is very light and compact. Halved Morse-type taper pins are introduced in its center so that the compression of the taper pins against the specimen becomes very strong without any accompanying slippage. The displacement of vibration is concurrently detected by a noncontacting displacement meter (the present resolution is 0.2 μm).

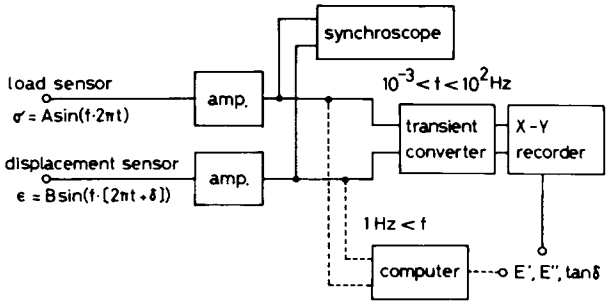

Fig. 5. Electric schematic for the recording device.

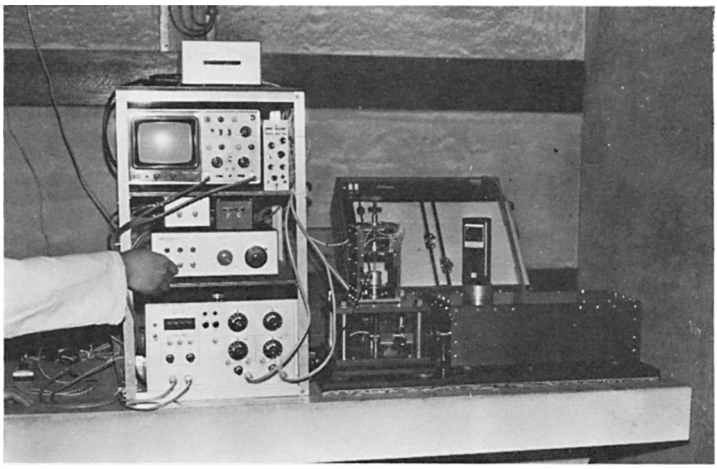

(a)

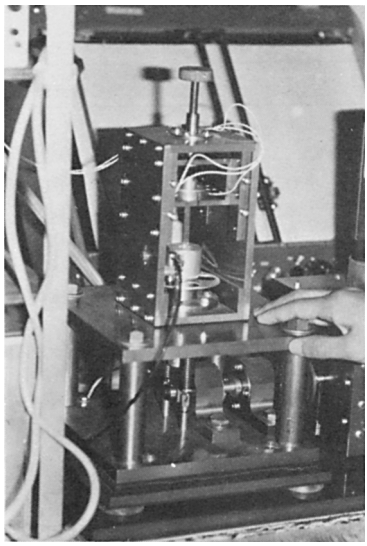

(b)

Fig. 6. (a) General view and (b) main part of the instrument.

Recording Device

The electrical outputs from the load cell and noncontacting displacement meter were amplified and led to the vertical and horizontal axes of the synchroscope (Fig. 5). This is useful for the regular watching of the vibrational state and the distribution of tension in the specimen. When the frequency is higher (more than 1 Hz), the signals of load and displacement are led into a computing circuit where the values of E', E'', and tan δ (with a precision of 0.002) can be directly calculated. Similar treatments have already been developed by other workers.[1-4] However, this circuit cannot be generally applied to the frequency range lower than 1 Hz. In this case, the signals of load and displacement are temporarily memorized in the transient converter and are reproduced on the X–Y recorder under a slower and constant time base. From the recorded Lis-

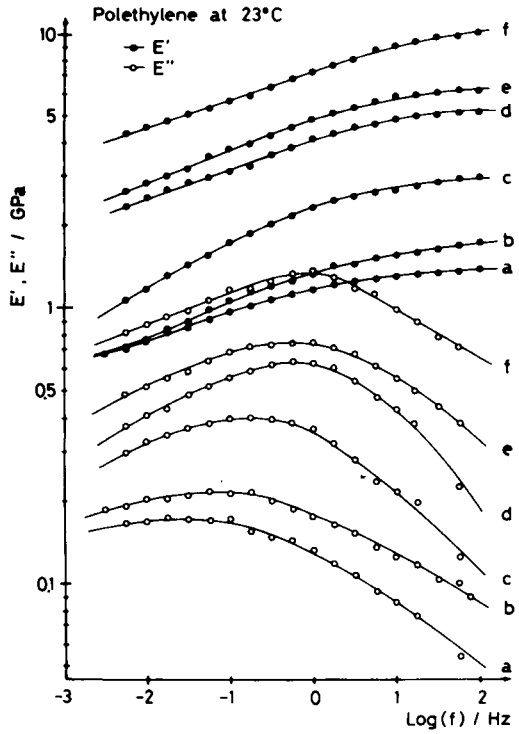

Fig. 7. Frequency dispersion of E' (●) and E'' (○) at 23°C for polyethylene with various degrees of extension: increase in orientation from (*a*) to (*f*).

sajous' figure (Fig. 1), the values of $2A$, $2B$, $2a$, $2b$, and θ can be obtained. The relationship between these parameters and the phase lag δ is represented by eq. (12):

$$\delta = \sin^{-1}\left[\frac{a^2b^2}{A^2(a^2\sin^2\theta + b^2\cos^2\theta)}\right]^{1/2} \tag{12}$$

In high precision, the following approximation can exist:

$$\delta = \sin^{-1}\frac{b(A^2 + B^2)^{1/2}}{AB} \tag{13}$$

Consequently, the necessary reading parameters from the Lissajous' figure are only three ($2A$, $2B$, and $2b$). Then, the values of δ (with a precision 0.3°), E', and E'' are easily calculated from eqs. (13), (5), and (6). Figure 6 shows the photographs of the fabricated viscoelastometer.

INSTRUMENT PERFORMANCE

The dynamic mechanical properties serve as a useful tool to study the variation of relaxational motions induced by structural changes. Since polymer chains are very anisotropic, the change in physical properties becomes remarkable by orientational procedures. Therefore, this instrument is especially suited for drawn samples. In the case of dynamic dielectric measurements, the frequency dispersion analysis exercises little power because the sinusoidal load voltage hardly occurs in the drawing direction.

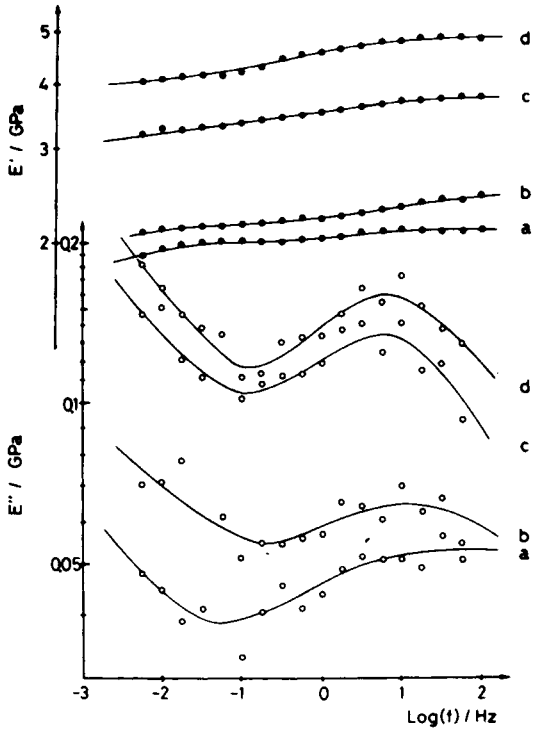

Fig. 8. Frequency dispersion of E' and E'' at 23°C for poly(ethylene terephthalate) with various degrees of extension: increase in orientation from (*a*) to (*d*).

In this report, two polymer sheets [polyethylene, PE, and poly(ethylene terephthalate), PET] with various degrees of extension were tested. All specimens used are listed in Table I. Since the specimen length (L) was fixed at 58 mm and the amplitude of displacement (B) at 100 μm, the maximum strain became 0.34%. The measurements for the frequency dispersion of E' and E'' were performed in the range from 10^{-3} to 10^{2} Hz at constant temperature of 23°C. Figure 7 shows the experimental results for PE. As the degree of orientation (detected by birefringence) was increased, the dynamic tensile storage modulus E' increased monotonously. The peak observed at 1.8×10^{-2} Hz in the dynamic tensile loss modulus E'' of the undrawn PE has been assigned to grain-boundary relaxation due to slippage between lamellae.[5] Then, it was expected that the noncrystalline regions between lamellae must be gradually tightened by the increase in orientation and its peak shifts to a higher frequency region. This anticipation was clearly demonstrated by the results (Fig. 7).

Figure 8 shows the experimental results for PET. The primary dispersion exists in a frequency lower than 10^{-3} Hz at 23°C. At this temperature, the location of the β relaxation has been dielectrically assigned to approximately 10^{5} Hz. It is not probable that the grain (crystallite)-boundary relaxation participates in the peak since the quantity of crystallite was relatively small and a shift of the peak frequency to a higher region by the increase in orientation was not observed.

The thicknesses of the above samples were from 30 to 300 μm. The range of the measurable modulus depends on the sample size. The present apparatus

measured the dynamic moduli of other polymer solids from 1 MPa (rubber) to 50 GPa (high modulus PE) at 23°C, using fixtures to clamp the samples with various cross sections.

CONCLUSIONS

A dynamic tensile viscoelastometer has been developed. The fabricated instrument enables us to measure continuous frequency dispersion of the dynamic mechanical properties of polymer solids in the range from 10^{-3} Hz to 10^{2} Hz with sufficient and clear sinusoidal driving force. Furthermore, it is relatively simple to operate and can be used in routine laboratory testing. For the measurement of temperature dispersion, a special air-circulating oven is used to control the temperature in the range from −20 to 80°C. The concurrent data in the wide range of frequency and temperature dispersions may give valuable information for the dynamic viscoelastic properties of polymer solids.

The authors would like to thank the machine shop employees of the university for help in manufacturing the instrument.

References

1. M. Yoshino and M. Takayanagi, *J. Japan Soc. Test. Mater.*, **8,** 330 (1959).
2. E. Fukada and M. Date, *J. Japan Soc. Test. Mater.*, **10,** 344 (1961).
3. A. S. Kenyon, W. A. Grote, D. A. Wallace, and McC. Rayford, *J. Macromol. Sci.-Phys.*, **B13,** 553 (1977).
4. A. F. Yee and M. T. Takemori, *J. Appl. Polym. Sci.*, **21,** 2597 (1977).
5. Y. Wada, *The Solid State Physics of Polymer*, 1st ed., Baifukan, Tokyo, 1974.

Received January 26, 1981
Accepted June 30, 1981